Ultrasound for the Diagnosis of Biliary Atresia

Subjects: Gastroenterology & Hepatology

Contributor: Luyao Zhou

Biliary atresia is an aggressive liver disease of infancy and can cause death without timely surgical intervention. Early diagnosis of biliary atresia is critical to the recovery of bile drainage and long-term transplant-free survival. Ultrasound is recommended as the initial imaging strategy for the diagnosis of biliary atresia. Numerous ultrasound features have been proved helpful for the diagnosis of biliary atresia. In recent years, with the help of new technologies such as elastography ultrasound, contrast-enhanced ultrasound and artificial intelligence, the diagnostic performance of ultrasound has been significantly improved.

Keywords: biliary atresia ; imaging ; conventional ultrasound ; elastography ; percutaneous cholecystocholangiography ; artificial intelligence

1. Introduction

Biliary atresia (BA) is a severe obliterative fibrosing cholangiopathy of infancy, with a worldwide prevalence ranging from 1 in 5000 to 19,000 livebirths [1][2][3]. If left untreated, BA can lead to progressive liver cirrhosis, and finally result in death from hepatic failure by age 2 years [4]. Kasai portoenterostomy (KPE) is the primary treatment to restore bile flow for patients with BA. The prognosis of KPE for patients less than 60 days is significantly better than that for those more than 60 days [5]. Liver transplantation is consequently performed if KPE fails to restore bile flow or other severe liver-related events occur. Thus, early diagnosis of BA is extremely critical, as early surgical intervention is required to achieve long-term transplant-free survival.

2. Conventional Ultrasound

Conventional US is comprised of grey scale US and color Doppler US. With the help of constantly updated US equipment, the US features can be observed clearly better than ever before. High-frequency ultrasound (>10 MHz) is suggested for grey scale US and color Doppler to achieve the best spatial resolution. Numerous US features, especially the combination of gallbladder abnormalities and the triangular cord (TC) sign [6], have been proved helpful for diagnosing BA. Either of the two is positive, the infant should receive surgical exploration or cholangiography for the exclusion of BA.

2.1. Gallbladder Abnormalities

Gallbladder abnormality is the earliest and most widely used US feature for diagnosing BA, usually with both sensitivity and specificity more than 90% [6][7][8]. On US, a normal gallbladder is displayed with a complete and smooth hyperechoic mucosal lining, regardless of whether the gallbladder lumen is completely filled or not. Due to congenital dysplasia of the gallbladder, the size or the morphology of the gallbladder of infant with BA is usually abnormal. The definitions of gallbladder abnormalities have varied among different studies [7][8][9][10][11][12]. The length of the gallbladder, the integrity of the mucosal lining, and the degree of contraction of the gallbladder after feeding had all been reported to identify BA [7][8][9][10][11][12].

Combining the experience of our center and the results of previous studies, a gallbladder classification scheme was proposed in 2015 for the diagnosis of BA [12], including four types of gallbladders: Type I, dysplastic gallbladder, in which the gallbladder was not detected; Type II, unfilled gallbladder, in which a gallbladder was detected with incompletely filled lumen and with smooth and complete hyperechogenic mucosal lining (**Figure 1**a); Type III, small gallbladder, in which a gallbladder was detected with a fully filled lumen and the length of the lumen <1.5 cm (**Figure 1**b); Type IV, in which a gallbladder was detected with a fully filled lumen and the length of the lumen more than 1.5 cm (**Figure 1**c,d). For type IV, the maximum length and width of the gallbladder were measured from inner wall to inner wall (**Figure 1**d), and the length-to-width ratio was calculated. In particular, when measuring the length of the gallbladder, it is necessary to perform a segmental measurement according to the meandering of the gallbladder. An abnormal gallbladder was defined as type I, type III, and type IV with length-to-width ratios of >5.2 (**Figure 1**c), and used to predict BA. A normal gallbladder was

defined as type II and type IV gallbladders with length-to-width ratios of ≤5.2 (**Figure 1**d), and used to predict non-BA. This classification scheme yielded a sensitivity of 86.8% and a specificity of 90.3% [12].

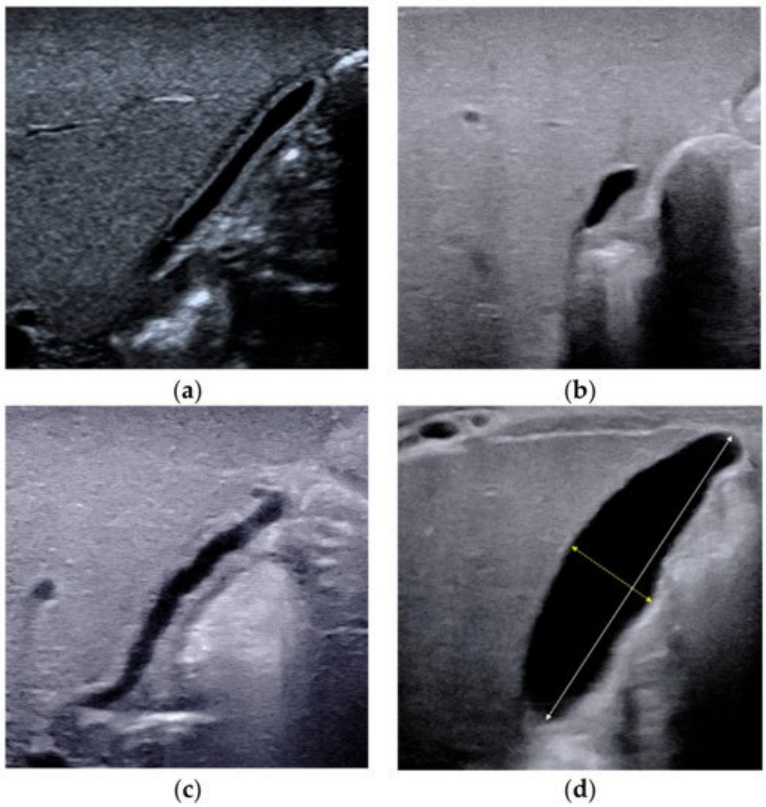

Figure 1. Different types of gallbladders detected by conventional ultrasound. (**a**) Type II gallbladder in non-BA. (**b**) Type III gallbladder in BA. (**c**) Type IV gallbladder with length-to-width ratios of >5.2 in BA. (**d**) Type IV gallbladder with length-to-width ratios of ≤5.2 in non-BA. The maximum lumen length and width should be measured from inner wall to inner wall.

2.2. Triangular Cord Sign

The TC thickness is very sensitive in the identification of BA [12][13][14][15]. It was firstly defined as the triangular or tubular-shaped echogenic density above the portal vein on a transverse or longitudinal image by Choi et al. [14] in 1996. Subsequent studies had also proved that TC sign was a helpful indicator for diagnosing BA [6][13][15]. However, the location and the cut-off value of TC thickness in different studies varied. The most frequently used TC sign is defined as the echogenic area >4 mm including hepatic artery (HA) (**Figure 2**a), located at the right portal vein on a longitudinal scan [13]. Patients with a thickness value less than 4 mm (**Figure 2**b) were deemed as without BA.

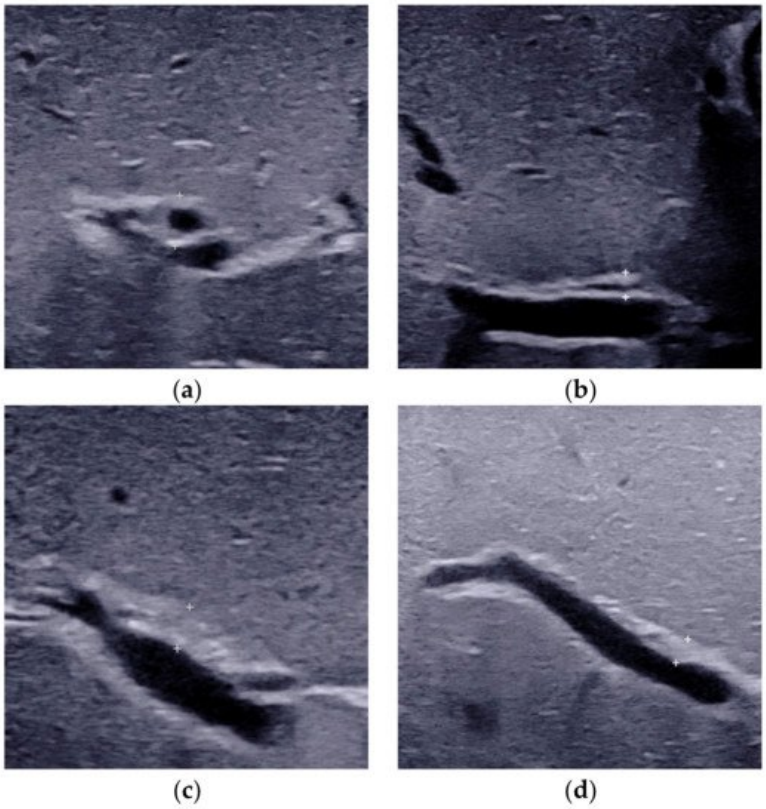

Figure 2. The triangular cord thickness measured above the anterior branch of the right portal vein on a longitudinal image. (**a**) The TC thickness >4.0mm including HA in BA. (**b**) The TC thickness <4.0 mm including HA in non-BA. (**c**) The TC thickness >2.0 mm not including HA in BA. (**d**) The TC thickness <2.0 mm not including HA in non-BA. TC, triangular cord; HA, hepatic artery; BA, biliary atresia.

2.3. Porta Hepatis Macro- or Microcyst

The presence of the porta hepatis macrocyst (**Figure 3**a) or microcyst (**Figure 3**b) is a specific sign for BA [16][17]. Macrocyst was defined as the cyst with a diameter >5 mm located in the hepatic pedicle [16][17], while microcyst was defined as the cystv ≤5 mm in diameter in front of the right portal vein at the hepatic portal [16]. Color Doppler can help distinguish cysts from blood vessels. When the porta hepatis cyst is detected in infants with conjugated hyperbilirubinemia on US scan, BA should be highly suspected. In addition, most of BA with microcyst is type III BA, while some of BA with macrocyst is type I BA [18].

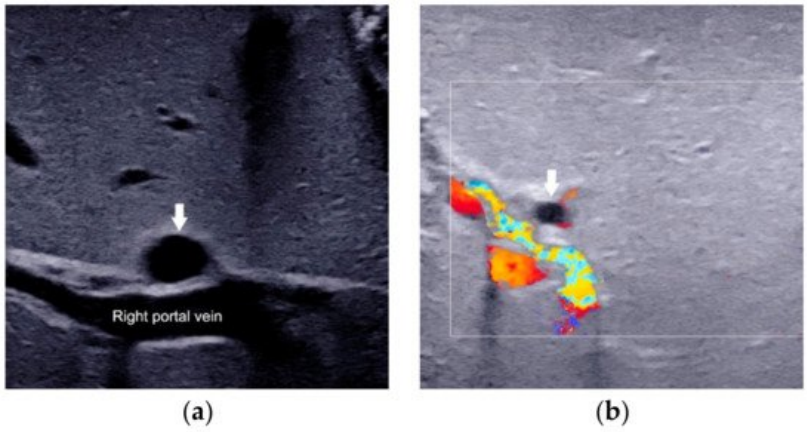

Figure 3. Porta hepatis macrocyst (**a**) and microcyst (**b**) in infants with biliary atresia.

2.4. Enlarged Hepatic Hilar Lymph Node (LN)

The presence of enlarged hepatic hilar LN, which was defined as the LN located at the porta hepatis and around the hepatoduodenal ligament (**Figure 4**), is also useful for the diagnosis of BA [19]. The optimal cutoff value was 6.0 mm for the length of LN in the identification of BA, which yielded a sensitivity and specificity of 91.1% and 82.9%, respectively. Combined hepatic hilar LN with gallbladder classification and TC thickness, the sensitivity could even reach 100%. However, the value of hepatic hilar LN was tested in only a single institution. A validation in independent population by other investigators is necessary.

Figure 4. The presence of enlarged hepatic hilar lymph node (calipers) in infants with biliary atresia.

2.5. Other Helpful US Features

Several studies have shown that the diameter of HA in infants with BA (**Figure 5**a) is larger than that of non-BA (**Figure 5**b) [12][20][21][22][23]. Woo et al. [20] proposed an optimal cutoff value of 1.5 mm for HA diameter in the diagnosis of BA, which yielded a sensitivity of 92% and specificity of 87%. However, the mean diameter of HA between BA and non-BA groups varies greatly in different studies [12][20][21][22][23]. According to reports, the mean HA diameter of BA was between 2.1 mm to 2.5 mm, while the diameter of non-BA was between 1.5 mm to 1.9 mm [12][21][22][23]. Obviously, 1.5 mm is not an optimal cutoff value in the diagnosis of BA. Furthermore, the measurement of the diameter of HA is hard to standardize. Due to the unsatisfactory consistency of diameter of HA in different studies, it is not yet a reliable diagnostic indicator in predicting BA.

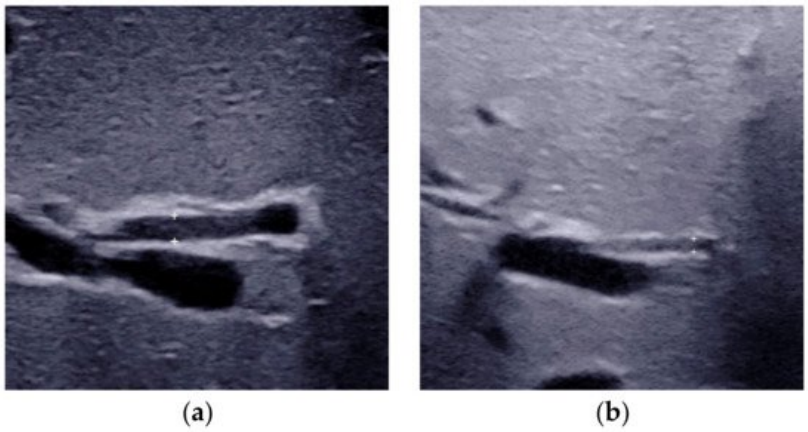

Figure 5. Hepatic artery measurement images of infants with (**a**) and without biliary atresia (**b**).

The presence of hepatic subcapsular flow (**Figure 6**) is a sign of hyperplastic and hypertrophic changes in branches of the hepatic artery, with the sensitivity ranged from 96.3% to 100% and the specificity ranged from 86% to 96.7% in predicting BA [21][22][23].

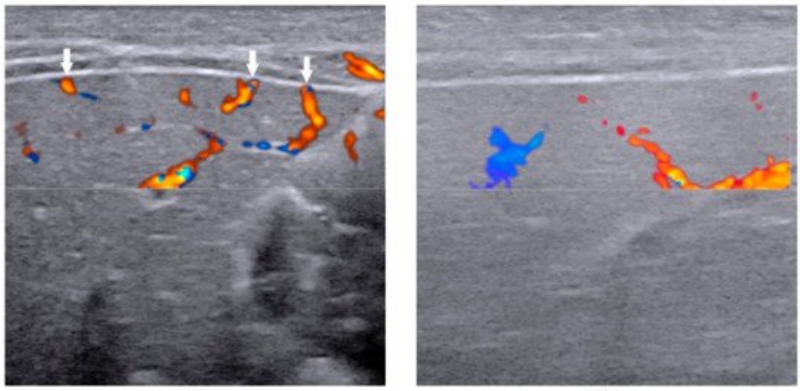

Figure 6. The presence of hepatic subcapsular flow (arrows) in biliary atresia (**a**) and the absence of hepatic subcapsular flow in non-biliary atresia (**b**).

3. Elastography

Elastography can be performed to quantify liver stiffness and fibrosis in infants with cholestasis [24][25][26] and to facilitate the differential diagnosis of BA [27][28][29][30][31][32][33][34][35][36][37]. With the development of elastography technology, various types of elastography have been reported for the diagnosis of BA.

Transient elastography (TE) is another type of quantitative elastography technology used to diagnose BA. A cut-off value of 7.7 kPa of TE yielded a sensitivity of 80% and specificity of 97% in infants younger than 90 days [32]. For the infants aged 91 to 180 days, a higher cutoff value of 8.8 kPa could yield higher diagnostic sensitivity (100%) and specificity (100%) [38]. However, the inability to choose different locations for the region of interest limits the clinical applicability of TE [39] in children.

Supersonic shear wave elastography (SSWE) is a recently developed elastography system based on high frame-rate shear wave technology. It is based on capturing shear wave speed propagation, which presents a map of the elasticity in one area and allows stiffness quantitative analysis [27][28][34]. In our previous study, the cutoff value of SSWE for differentiating BA (**Figure 7**a) from non-BA (**Figure 7**b) was determined to be ≥10.2 kPa, with AUC 0.790, sensitivity 81.4% and specificity 66.7% [27].

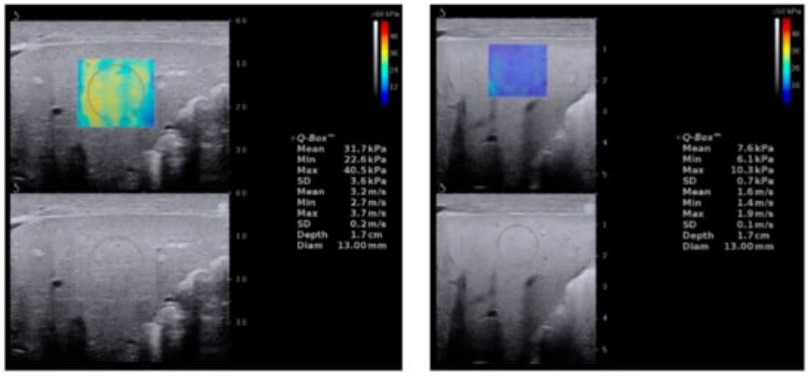

Figure 7. Liver stiffness measurement images of biliary atresia (**a**) and non-biliary atresia (**b**).

4. US-Guided Percutaneous Cholecystocholangiography with Microbubbles

For those infants with a persistent rise of direct bilirubin level but equivocal US results, US-guided percutaneous cholecystocholangiography (PCC) may be used as another less invasive alternative to laparoscopic cholangiography if their gallbladder is full [40][41][42]. As previously reported, the diagnostic performance of US-guided PCC was better than that of conventional US [40][41]. Furthermore, it was helpful to be used for preoperatively differentiating subtypes of BA.

Infants should be fasted for more than 4 h and then conventional US should be performed before US-guided PCC to ascertain the presence of a filled gallbladder that is potentially available for puncturing. Afterwards, general anesthesia is induced and US-guided PCC is performed with a linear transducer. After percutaneous puncture through the anterior wall of the gallbladder into the gallbladder lumen, the diluted microbubble contrast agent is injected via the puncture needle to

allow observation of the distribution of the contrast agent in the biliary system. BA is excluded if the gallbladder, common hepatic duct, common bile duct, and bowel are seen to fill with microbubble (**Figure 8**a). BA is confirmed if the common hepatic duct is invisible (**Figure 8**b).

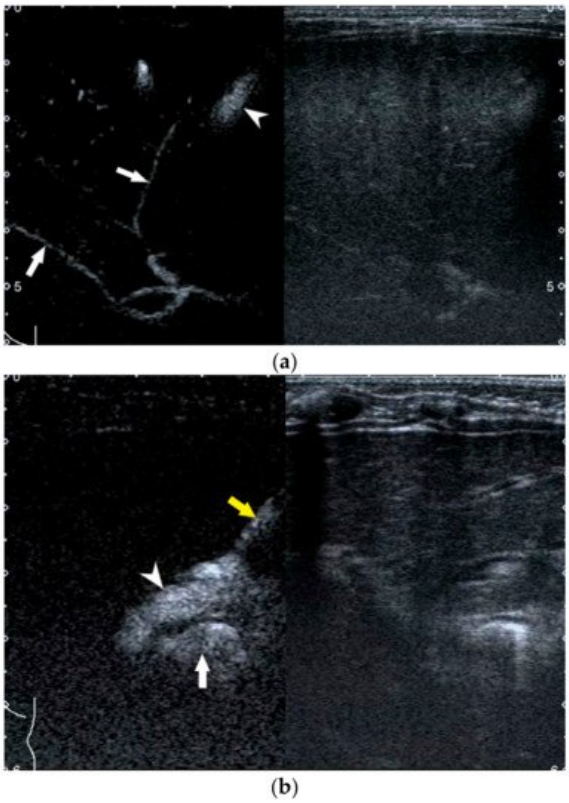

Figure 8. Image obtained at US-guided percutaneous cholecystocholangiography with microbubbles. (**a**) Gallbladder is filled with contrast material (arrowhead) and contrast material flows into intrahepatic bile ducts (arrows) in an infant without BA. (**b**) Contrast material flows along the puncture needle (yellow arrow) into the gallbladder (white arrowhead) and then into bowel (white arrow) in an infant with BA. No contrast material flows into the intrahepatic bile duct.

5. Artificial Intelligence Based on US Gallbladder Images

AI may have the potential to revolutionize BA diagnosis from US images particularly in rural area without relevant expertise.

Recently, an ensemble deep learning model from US gallbladder images has been developed, which adopted two types of effective AI techniques called deep convolutional neural networks (CNNs) and ensemble learning [43]. In this study, the training cohort was randomly separated into five complementary subsets, four of which were used each time to train a CNN, and the remaining subset was used for validation. Thus, five CNNs were trained with the training cohort and then the output predictions of these CNNs were averaged to predict the diagnosis of each test image, resulting in an ensemble deep learning model.

The ensemble deep learning model yielded a sensitivity 93.1% and specificity 93.9% on the external validation dataset, superior to that of three human experts [44]. With the help of the model, the performances of human experts with various levels were improved. It proves that AI can provide a solution to help radiologists improve their diagnosis of BA, particularly for the junior radiologists without relevant expertise.

It is worth trying that BA can be diagnosed through AI automatic detection and measurement of TC thickness, or through AI to extract more features from elastography images, not just through a single liver stiffness measurement value.

References

1. Chardot, C.; Carton, M.; Spire-Bendelac, N.; Le Pommelet, C.; Golmard, J.-L.; Auvert, B. Epidemiology of biliary atresia in France: A national study 1986–96. J. Hepatol. 1999, 31, 1006–1013.
2. Hsiao, C.-H.; Chang, M.H.; Chen, H.-L.; Lee, H.-C.; Wu, T.-C.; Lin, C.-C.; Yang, Y.-J.; Chen, A.-C.; Tiao, M.-M.; Lau, B.-H.; et al. Universal screening for biliary atresia using an infant stool color card in Taiwan. Hepatology 2007, 47, 1233–

1240.

3. McKiernan, P.J.; Baker, A.J.; A Kelly, D. The frequency and outcome of biliary atresia in the UK and Ireland. Lancet 2000, 355, 25–29.
4. Hartley, J.L.; Davenport, M.; A Kelly, D. Biliary atresia. Lancet 2009, 374, 1704–1713.
5. Shneider, B.L.; Brown, M.B.; Haber, B.; Whitington, P.F.; Schwarz, K.; Squires, R.; Bezerra, J.; Shepherd, R.; Rosenthal, P.; Hoofnagle, J.H.; et al. A multicenter study of the outcome of biliary atresia in the United States, 1997 to 2000. J. Pediatr. 2006, 148, 467–474.e1.
6. Zhou, L.; Shan, Q.; Tian, W.; Wang, Z.; Liang, J.; Xie, X. Ultrasound for the Diagnosis of Biliary Atresia: A Meta-Analysis. AJR Am. J. Roentgenol. 2016, 206, W73–W82.
7. Farrant, P.; Meire, H.B.; Mieli-Vergani, G. Ultrasound features of the gall bladder in infants presenting with conjugated hyperbilirubinaemia. Br. J. Radiol. 2000, 73, 1154–1158.
8. Humphrey, T.M.; Stringer, M.D. Biliary Atresia: US Diagnosis. Radiology 2007, 244, 845–851.
9. Kendrick, A.P.A.T.; Phua, K.B.; Ooi, B.C.; Tan, C.E.L. Biliary atresia: Making the diagnosis by the gallbladder ghost triad. Pediatr. Radiol. 2003, 33, 311–315.
10. Ikeda, S.; Sera, Y.; Akagi, M. Serial ultrasonic examination to differentiate biliary atresia from neonatal hepatitis—Special reference to changes in size of the gallbladder. Eur. J. Pediatrics 1989, 148, 396–400.
11. McGahan, J.P.; E Phillips, H.; Cox, K.L. Sonography of the normal pediatric gallbladder and biliary tract. Radiology 1982, 144, 873–875.
12. Zhou, L.-Y.; Wang, W.; Shan, Q.-Y.; Liu, B.-X.; Zheng, Y.-L.; Xu, Z.-F.; Xu, M.; Pan, F.-S.; Lu, M.-D.; Xie, X.-Y. Optimizing the US Diagnosis of Biliary Atresia with a Modified Triangular Cord Thickness and Gallbladder Classification. Radiology 2015, 277, 181–191.
13. Lee, H.-J.; Lee, S.-M.; Park, W.-H.; Choi, S.-O. Objective Criteria of Triangular Cord Sign in Biliary Atresia on US Scans. Radiology 2003, 229, 395–400.
14. Choi, S.-O.; Park, W.-H.; Lee, H.-J.; Woo, S.-K. ‘Triangular cord’: A sonographic finding applicable in the diagnosis of biliary atresia. J. Pediatr. Surg. 1996, 31, 363–366.
15. Park, W.-H.; Choi, S.-O.; Lee, H.-J.; Kim, S.-P.; Zeon, S.-K.; Lee, S.-L. A new diagnostic approach to biliary atresia with emphasis on the ultrasonographic triangular cord sign: Comparison of ultrasonography, hepatobiliary scintigraphy, and liver needle biopsy in the evaluation of infantile cholestasis. J. Pediatr. Surg. 1997, 32, 1555–1559.
16. Koob, M.; Pariente, D.; Habes, D.; Ducot, B.; Adamsbaum, C.; Franchi-Abella, S. The porta hepatis microcyst: An additional sonographic sign for the diagnosis of biliary atresia. Eur. Radiol. 2017, 27, 1812–1821.
17. Caponcelli, E.; Knisely, A.S.; Davenport, M. Cystic biliary atresia: An etiologic and prognostic subgroup. J. Pediatr. Surg. 2008, 43, 1619–1624.
18. Shan, Q.-Y.; Liu, B.-X.; Zhong, Z.-H.; Chen, H.-D.; Guo, Y.; Xie, X.-Y.; Zhou, W.-Y.; Jiang, H.; Zhou, L.-Y. The Prognosis of Type III Biliary Atresia with Hilar Cyst. Indian J. Pediatr. 2021, 88, 650–655.
19. Weng, Z.; Zhou, L.; Wu, Q.; Zhou, W.; Ma, H.; Fang, Y.; Dang, T.; Liu, M. Enlarged hepatic hilar lymph node: An additional ultrasonographic feature that may be helpful in the diagnosis of biliary atresia. Eur. Radiol. 2019, 29, 6699–6707.
20. Kim, W.S.; Cheon, J.-E.; Youn, B.J.; Yoo, S.-Y.; Kim, W.Y.; Kim, I.-O.; Yeon, K.M.; Seo, J.K.; Park, K.-W. Hepatic Arterial Diameter Measured with US: Adjunct for US Diagnosis of Biliary Atresia. Radiology 2007, 245, 549–555.
21. El-Guindi, M.A.-S.; Sira, M.M.; Sira, A.M.; Salem, T.A.-H.; El-Abd, O.L.; Konsowa, H.A.-S.; El-Azab, D.S.; Allam, A.A.-H. Design and validation of a diagnostic score for biliary atresia. J. Hepatol. 2014, 61, 116–123.
22. El-Guindi, M.A.-S.; Sira, M.M.; Konsowa, H.A.-S.; El-Abd, O.L.; Salem, T.A.-H. Value of hepatic subcapsular flow by color Doppler ultrasonography in the diagnosis of biliary atresia. J. Gastroenterol. Hepatol. 2013, 28, 867–872.
23. Lee, M.S.; Kim, M.-J.; Lee, M.-J.; Yoon, C.S.; Han, S.J.; Oh, J.-T.; Park, Y.N. Biliary Atresia: Color Doppler US Findings in Neonates and Infants. Radiology 2009, 252, 282–289.
24. Chen, H.; Zhou, L.; Liao, B.; Cao, Q.; Jiang, H.; Zhou, W.; Wang, G.; Xie, X. Two-Dimensional Shear Wave Elastography Predicts Liver Fibrosis in Jaundiced Infants with Suspected Biliary Atresia: A Prospective Study. Korean J. Radiol. 2021, 22, 959–969.
25. Galina, P.; Alexopoulou, E.; Mentessidou, A.; Mirilas, P.; Zellos, A.; Lykopoulou, L.; Patereli, A.; Salpasaranis, K.; Kelekis, N.L.; Zarifi, M. Diagnostic accuracy of two-dimensional shear wave elastography in detecting hepatic fibrosis in

children with autoimmune hepatitis, biliary atresia and other chronic liver diseases. Pediatr. Radiol. 2021, 51, 1358–1368.

26. Gao, F.; Chen, Y.-Q.; Fang, J.; Gu, S.-L.; Li, L.; Wang, X.-Y. Acoustic Radiation Force Impulse Imaging for Assessing Liver Fibrosis Preoperatively in Infants with Biliary Atresia: Comparison with Liver Fibrosis Biopsy Pathology. J. Ultrasound Med. Off. J. Am. Inst. Ultrasound Med. 2017, 36, 1571–1578.
27. Zhou, L.-Y.; Jiang, H.; Shan, Q.-Y.; Chen, D.; Lin, X.-N.; Liu, B.-X.; Xie, X.-Y. Liver stiffness measurements with supersonic shear wave elastography in the diagnosis of biliary atresia: A comparative study with grey-scale US. Eur. Radiol. 2017, 27, 3474–3484.
28. Wang, X.; Qian, L.; Jia, L.; Bellah, R.; Wang, N.; Xin, Y.; Liu, Q. Utility of Shear Wave Elastography for Differentiating Biliary Atresia from Infantile Hepatitis Syndrome. J. Ultrasound Med. Off. J. Am. Inst. Ultrasound Med. 2016, 35, 1475–1479.
29. Liu, Y.; Peng, C.; Wang, K.; Wu, D.; Yan, J.; Tu, W.; Chen, Y. The utility of shear wave elastography and serum biomarkers for diagnosing biliary atresia and predicting clinical outcomes. Eur. J. Pediatrics 2021, 30, 1–10.
30. Sandberg, J.K.; Sun, Y.; Ju, Z.; Liu, S.; Jiang, J.; Koci, M.; Rosenberg, J.; Rubesova, E.; Barth, R.A. Ultrasound shear wave elastography: Does it add value to gray-scale ultrasound imaging in differentiating biliary atresia from other causes of neonatal jaundice? Pediatr. Radiol. 2021, 51, 1654–1666.
31. Thumar, V.; Squires, J.H.; Spicer, P.J.; Robinson, A.L.; Chan, S.S. Ultrasound Elastography Applications in Pediatrics. Ultrasound Q. 2018, 34, 199–205.
32. Wu, J.-F.; Lee, C.-S.; Lin, W.-H.; Jeng, Y.-M.; Chen, H.-L.; Ni, Y.-H.; Hsu, H.-Y.; Chang, M.-H. Transient elastography is useful in diagnosing biliary atresia and predicting prognosis after hepatoportoenterostomy. Hepatology 2018, 68, 616–624.
33. Chen, S.; Liao, B.; Zhong, Z.; Zheng, Y.; Liu, B.; Shan, Q.; Xie, X.; Zhou, L. Supersonic shearwave elastography in the assessment of liver fibrosis for postoperative patients with biliary atresia. Sci. Rep. 2016, 6, 31057.
34. Leschied, J.R.; Dillman, J.R.; Bilhartz, J.; Heider, A.; Smith, E.A.; Lopez, M.J. Shear wave elastography helps differentiate biliary atresia from other neonatal/infantile liver diseases. Pediatr. Radiol. 2015, 45, 366–375.
35. Dillman, J.R.; DiPaola, F.W.; Smith, S.J.; Barth, R.A.; Asai, A.; Lam, S.; Campbell, K.M.; Bezerra, J.A.; Tiao, G.M.; Trout, A. Prospective Assessment of Ultrasound Shear Wave Elastography for Discriminating Biliary Atresia from other Causes of Neonatal Cholestasis. J. Pediatr. 2019, 212, 60–65.e3.
36. Hanquinet, S.; Courvoisier, D.S.; Rougemont, A.-L.; Dhouib, A.; Rubbia-Brandt, L.; Wildhaber, B.E.; Merlini, L.; McLin, V.A.; Anooshiravani, M. Contribution of acoustic radiation force impulse (ARFI) elastography to the ultrasound diagnosis of biliary atresia. Pediatr. Radiol. 2015, 45, 1489–1495.
37. Liu, Y.; Ni, X.; Pan, Y.; Luo, H. Comparison of the diagnostic value of virtual touch tissue quantification and virtual touch tissue imaging quantification in infants with biliary atresia. Int. J. Clin. Pr. 2021, 75, e13860.
38. Boo, Y.; Chang, M.; Jeng, Y.; Peng, S.; Hsu, W.; Lin, W.; Chen, H.; Ni, Y.; Hsu, H.; Wu, J. Diagnostic Performance of Transient Elastography in Biliary Atresia among Infants with Cholestasis. Hepatol. Commun. 2021, 5, 882–890.
39. Goldschmidt, I.; Streckenbach, C.; Dingemann, C.; Pfister, E.D.; di Nanni, A.; Zapf, A.; Baumann, U. Application and Limitations of Transient Liver Elastography in Children. J. Pediatr. Gastroenterol. Nutr. 2013, 57, 109–113.
40. Zhou, L.-Y.; Chen, S.-L.; Chen, H.-D.; Huang, Y.; Qiu, Y.-X.; Zhong, W.; Xie, X.-Y. Percutaneous US-guided Cholecystocholangiography with Microbubbles for Assessment of Infants with US Findings Equivocal for Biliary Atresia and Gallbladder Longer than 1.5 cm: A Pilot Study. Radiology 2018, 286, 1033–1039.
41. Lee, S.Y.; Kim, G.C.; Choe, B.-H.; Ryeom, H.K.; Jang, Y.-J.; Kim, H.J.; Park, J.Y.; Cho, S.-M. Efficacy of US-guided Percutaneous Cholecystocholangiography for the Early Exclusion and Type Determination of Biliary Atresia. Radiology 2011, 261, 916–922.
42. Treem, W.R.; Grant, E.E.; Barth, K.H.; Kramers, P.W. Ultrasound Guided Percutaneous Cholecystocholangiography for Early Differentiation of Cholestatic Liver Disease in Infants. J. Pediatr. Gastroenterol. Nutr. 1988, 7, 347–352.
43. Zhou, W.; Yang, Y.; Yu, C.; Liu, J.; Duan, X.; Weng, Z.; Chen, D.; Liang, Q.; Fang, Q.; Zhou, J.; et al. Ensembled deep learning model outperforms human experts in diagnosing biliary atresia from sonographic gallbladder images. Nat. Commun. 2021, 12, 1259.
44. Buda, M.; Wildman-Tobriner, B.; Hoang, J.K.; Thayer, D.; Tessler, F.N.; Middleton, W.D.; Mazurowski, M.A. Management of Thyroid Nodules Seen on US Images: Deep Learning May Match Performance of Radiologists. Radiology 2019, 292, 695–701.